Supplementary Information

Shaping liquid films by dielectrophoresis

Israel Gabay[1], Federico Paratore[2], Evgeniy Boyko[1,3], Antonio Ramos[4], Amir D. Gat[1*], Moran Bercovici[1*]

[1]*Faculty of Mechanical Engineering, Technion–Israel Institute of Technology, Haifa 3200003, Israel.*

[2]*IBM Research Europe, Säumerstrasse 4 CH–8803 Rüschlikon, Zurich, Switzerland.*

[3]*Department of Mechanical and Aerospace Engineering, Princeton University, Princeton, NJ 08544, USA.*

[4]*Depto. Electrónica y Electromagnetismo, Facultad de Física, Universidad de Sevilla, Calle San Fernando, 4, Sevilla 41004, Spain.*

*Corresponding authors:

Moran Bercovici, mberco@technion.ac.il and Amir D. Gat, amirgat@technion.ac.il

Received:----; Revised:----; Accepted:-----;

Keywords: Dielectrophoresis; fluid shaping; free-surface; microfabrication; optics.

1. Electric force distribution on the interface

Consider two immiscible fluids with dielectric permittivity ε_1 and ε_2 separated by an interface with a surface charge density σ_E, as illustrated in Fig. S1., We define $\hat{\mathbf{t}}_1$ and $\hat{\mathbf{t}}_2$ as the tangential unit vectors and $\hat{\mathbf{n}}$ as the normal unit vector to the interface pointing from the lower to the upper fluid.

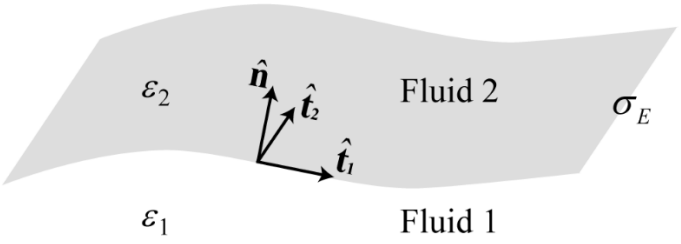

Fig. S1. *An illustration of an interface (gray surface) separating two immiscible fluids. The lower (fluid 1) and the upper (fluid 2) fluids have electric permittivity of ε_1 and ε_2, respectively, and σ_E is the surface charge density at the interface.*

To derive the electric stress acting at the interface, we start from the Maxwell stress tensor (Melcher, 1981; Stratton, 1941),

$$\mathbf{T}_{ij} = \varepsilon\left(E_i E_j - \frac{1}{2}\delta_{ij} E_k E_k \left(1 - \frac{\rho}{\varepsilon}\frac{\partial \varepsilon}{\partial \rho} \right) \right), \qquad [S1.1]$$

where ε is the fluid permittivity, E_i is the i component of the electric field at each point, and δ_{ij} is the Kronecker delta. The Maxwell stress tensor includes the Coulombic force contribution (the force on free charges), the dielectric force contribution due to permittivity gradients, and the electrostriction force contribution. The electrical stress (force distribution) acting on the interface can be written as $\mathbf{f} = \left(\mathbf{T}_2 - \mathbf{T}_1\right)\cdot\hat{\mathbf{n}}$, where $\mathbf{T}_1$ and $\mathbf{T}_2$ are the Maxwell stress tensor contributions from the lower and the upper sides of the interface, respectively.
The explicit expression for the force distribution at the interface is therefore,

$$\mathbf{f} = \frac{1}{2}\left[\varepsilon_2\left(E_{2,n}^2 - \left|\mathbf{E}_{2,\mathbf{t}}\right|^2 \right) + \varepsilon_1\left(\left|\mathbf{E}_{1,\mathbf{t}}\right|^2 - E_{1,n}^2 \right) + \left|\mathbf{E}_2\right|^2 \frac{\rho_2}{\varepsilon_2}\left(\frac{\partial \varepsilon}{\partial \rho}\right)_2 - \left|\mathbf{E}_1\right|^2 \frac{\rho_1}{\varepsilon_1}\left(\frac{\partial \varepsilon}{\partial \rho}\right)_1 \right]\hat{\mathbf{n}} + \varepsilon_2 \mathbf{E}_{2,\mathbf{t}} E_{2,n} - \varepsilon_1 \mathbf{E}_{1,\mathbf{t}} E_{1,n}$$

,[S1.2]

where $\mathbf{E}_1$ and $\mathbf{E}_2$ are the electric fields at the lower and the upper sides of the interface, respectively, $\mathbf{E}_{1,\mathbf{t}} \equiv \mathbf{E}_1 - E_{1,n}\hat{\mathbf{n}}$ and $\mathbf{E}_{2,\mathbf{t}} \equiv \mathbf{E}_2 - E_{2,n}\hat{\mathbf{n}}$ are the tangential components of the electric field, and $E_{1,n}$ and $E_{2,n}$ are the normal components of the electric field. We note that in the manuscript we marked the bottom fluid with subscript f for fluid, and the upper fluid with the subscript a for the air, here we kept them fluid 1 and fluid 2 to present the more general case of two general fluids.

Using the relations of the electric field components at the interface, the continuity of the tangential component of the electric field $\mathbf{E}_{1,\mathbf{t}} = \mathbf{E}_{2,\mathbf{t}}$, and the jump condition relating the normal components of the displacement field to the surface charge distribution at the interface, $\varepsilon_2 E_{2,n} - \varepsilon_1 E_{1,n} = \sigma_E$, we can express the tangential component of the electric force distribution at the interface as,

$$\mathbf{f}\cdot\begin{pmatrix}\mathbf{t_1}\\ \mathbf{t_2}\end{pmatrix}=\varepsilon_2\mathbf{E_{2,t}}E_{2,n}-\varepsilon_1\mathbf{E_{1,t}}E_{1,n}=\mathbf{E_{1,t}}\left(\varepsilon_2E_{2,n}-\varepsilon_1E_{1,n}\right)=\mathbf{E_{1,t}}\sigma_E=\mathbf{E_t}\sigma_E\,, \qquad [S1.3]$$

where $\mathbf{E_t}\equiv\mathbf{E_{1,t}}=\mathbf{E_{2,t}}$.

For the normal component of the force distribution at the interface, we use the same relations for the normal and tangential electric field, and after some algebraic manipulations we obtain,

$$\begin{aligned}\mathbf{f}\cdot\hat{\mathbf{n}}&=\frac{1}{2}\left[\varepsilon_2\left(E_{2,n}^2-\left|\mathbf{E_{2,t}}\right|^2\right)+\varepsilon_1\left(\left|\mathbf{E_{1,t}}\right|^2-E_{1,n}^2\right)+\left|\mathbf{E_2}\right|^2\rho_2\left(\frac{\partial\varepsilon}{\partial\rho}\right)_2-\left|\mathbf{E_1}\right|^2\rho_1\left(\frac{\partial\varepsilon}{\partial\rho}\right)_1\right]=\\&=\frac{1}{2}\left[\left(\varepsilon_1\left|\mathbf{E_t}\right|^2+\varepsilon_2E_{2,n}^2\right)\left(1-\frac{\varepsilon_2}{\varepsilon_1}\right)-\frac{\sigma_E^2}{\varepsilon_1}+\frac{2\varepsilon_2E_{2,n}\sigma_E}{\varepsilon_1}+\left|\mathbf{E_2}\right|^2\rho_2\left(\frac{\partial\varepsilon}{\partial\rho}\right)_2-\left|\mathbf{E_1}\right|^2\rho_1\left(\frac{\partial\varepsilon}{\partial\rho}\right)_1\right]\end{aligned}. \qquad [S1.4]$$

Under the assumptions of an alternating current electric field at high frequency, such that the liquid acts as a dielectric, and isothermal conditions, implying that the liquid properties are uniform, there are not accumulation of free charges in the system, and particularly at the interface, i.e., $\sigma_E=0$. Therefore, there are no Coulombic force and the force distribution at the interface arises solely from the discontinuity in the permittivity and fluid's density at the interface,

$$\mathbf{f}=\frac{1}{2}\left[\left(\varepsilon_1\left|\mathbf{E_t}\right|^2+\varepsilon_2E_{2,n}^2\right)\left(1-\frac{\varepsilon_2}{\varepsilon_1}\right)+\left|\mathbf{E_2}\right|^2\rho_2\left(\frac{\partial\varepsilon}{\partial\rho}\right)_2-\left|\mathbf{E_1}\right|^2\rho_1\left(\frac{\partial\varepsilon}{\partial\rho}\right)_1\right]\hat{\mathbf{n}}\,. \qquad [S1.5]$$

Equation [S1.5] clearly shows that both the normal and tangential components of the electric field contribute to the normal component of the electrostatic force, although the force is only in the normal direction to the interface.

For convenience, we decompose the normal component of the force distribution at the interface into two terms. The first term is the dielectric force contribution, f_{DEP},

$$f_{DEP}=\frac{1}{2}\left[\left(\varepsilon_1\left|\mathbf{E_t}\right|^2+\varepsilon_2E_{2,n}^2\right)\left(1-\frac{\varepsilon_2}{\varepsilon_1}\right)\right], \qquad [S1.6]$$

and the second term is the electrostriction contribution f_{ES},

$$f_{ES}=\frac{1}{2}\left[\left|\mathbf{E_2}\right|^2\rho_2\left(\frac{\partial\varepsilon}{\partial\rho}\right)_2-\left|\mathbf{E_1}\right|^2\rho_1\left(\frac{\partial\varepsilon}{\partial\rho}\right)_1\right]. \qquad [S1.7]$$

In the main text, we use the expression for f_{DEP} and f_{ES} when writing the normal stress balance for calculating the shape of the liquid-air interface at a steady state.

2. Calculating the shape of the interface

Consider a two-dimensional fluidic chamber of length l and depth h_0 filled with a dielectric liquid with volume V_f, as illustrated in Fig. S2. The floor of the chamber contains at its center a pair of electrodes of width and gap l_e and negligible thickness (Fig. S2B). The dielectric permittivity of the fluid and of the air above it are ε_f and ε_a, respectively, and the surface tension of the fluid-air interface is γ. Assuming the fluid have a uniform permittivity, we modify the Young-Laplace equation (normal stress balance at the interface) to account for the DEP force distribution on the interface, and present the equation for the fluid's height in the chamber,

$$\frac{\gamma h''}{\left(1+h'^2\right)^{3/2}} - \rho_f g h + f_{DEP} = P\,, \qquad \text{[S2.1]}$$

where h is the fluid's height, g is the gravitational acceleration, ρ_f is the density of the liquid, P is a constant representing the pressure and can be determined from the boundary conditions, and primes represent differentiation with respect to x. Under the long-wave approximation (Leal, 2007; Oron et al., 1997), i.e., $\tilde{h}'^2 \ll 1$, we obtain the following linear equation for the shape of the interface,

$$\gamma h'' - \rho g h + f_{DEP} = P\,. \qquad \text{[S2.2]}$$

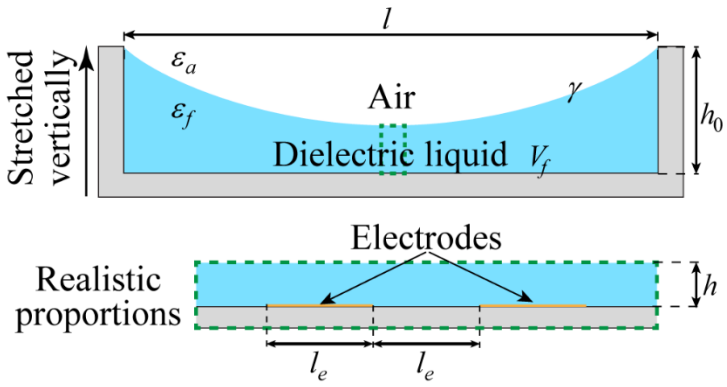

Fig. S2. *Two-dimensional illustration of the two-electrodes configuration and the relevant physical parameters used in modeling the system. (A) A dielectric liquid of volume V_f is placed in a chamber of length l and height h_0, forming a thin film wetting the chamber's floor and walls. Two surface electrodes of width and gap l_e, are located at the center of the chamber. The dielectric permittivity of the fluid and air above it are ε_f and ε_a, respectively, and the surface tension of the fluid-air interface is γ. (B) A closer view on the electrode region. Since the dimensions of the electrodes are significantly smaller than the size of the chamber, we assume an approximately constant height of the liquid film in this region for the purpose of electric field and force calculations.*

Using the following non-dimensional parameters, $h = h_0\eta,\quad x = \xi l/2$, we obtain the non-dimensional equation for the interface shape,

$$\eta'' - \mathrm{Bo}\,\eta + \frac{l^2}{4\gamma h_0} f_{DEP} = C_P\,, \qquad \text{[S2.3]}$$

where η is the non-dimensional height of the fluid, ξ is the non-dimensional spatial coordinate along the chamber, and $\mathrm{Bo} = \rho g l^2 / 4\gamma$ and C_P are the Bond number and the non-dimensional pressure constant. As presented in Fig. 3A, the numerically obtained DEP force distributions strongly resemble a Gaussian distribution. To facilitate an explicit expression for the deformation, we thus approximate the f_{DEP} as a Gaussian of width l_e, and an amplitude a set such that its total force matches F_{DEP},

$$f_{DEP} = a \exp\left(-\left(\frac{x}{l_e} \right)^2 \right), \quad a = \frac{F_{DEP}}{l_e \sqrt{\pi}\, \mathrm{erf}\left[l / 2 l_e \right]}. \qquad \text{[S2.4]}$$

Following the above assumption of Gaussian DEP force distribution, equation (S2.5) for the liquid shape under DEP actuation using pair of electrodes configuration takes the form,

$$\eta'' - \mathrm{Bo}\,\eta + \mathrm{DEP} \exp\left(-\frac{\xi^2}{c^2} \right) = C_P, \qquad \text{[S2.5]}$$

where $\mathrm{DEP} = \frac{a l^2}{4\gamma h_0}$ represents the non-dimensional amplitude of the force and $c = \frac{2 l_e}{l}$ represents the non-dimensional width of the Gaussian. We assume that the liquid is pinned at the edges of the chamber, $\eta(-1) = \eta(1) = 1$, providing two boundary conditions, and in addition require the total fluid volume to be conserved, $\int_{-1}^{1} \eta(\xi)\, d\xi = C_V$, providing the remaining conditions for resolving the pressure C_P.

The general solution for the shape of the interface, is given by,

$$\begin{aligned} \eta(\xi) = {} & \frac{e^{-\sqrt{Bo}\xi}}{4Bo\left(1 + e^{2\sqrt{Bo}}\right)} \left(4\left(Bo e^{\sqrt{Bo}} + e^{\sqrt{Bo}} C_P - e^{\sqrt{Bo}\xi} C_P - e^{\sqrt{Bo}(2+\xi)} C_P + e^{\sqrt{Bo}(1+2\xi)} \left(Bo + C_P \right) \right) \right. \\ & - \sqrt{Bo}\, c\, DEP\, e^{\frac{Boc^2}{4}} \sqrt{\pi} \left[\left(1 + e^{2\sqrt{Bo}\xi} \right) \mathrm{Erf}\left[\frac{1}{c} - \frac{\sqrt{Bo}c}{2} \right] - \left(e^{2\sqrt{Bo}} + e^{2\sqrt{Bo}(1+\xi)} \right) \mathrm{Erf}\left[\frac{1}{c} + \frac{\sqrt{Bo}c}{2} \right] + \right. , \\ & \left. \left. + \left(1 + e^{2\sqrt{Bo}} \right) \left(\mathrm{Erf}\left[\frac{\sqrt{Bo}c}{2} - \frac{\xi}{c} \right] + e^{2\sqrt{Bo}\xi} \mathrm{Erf}\left[\frac{\sqrt{Bo}c}{2} + \frac{\xi}{c} \right] \right) \right] \right) \end{aligned} \qquad \text{[S2.6]}$$

where the non-dimensional pressure term is,

$$\begin{aligned} C_P = {} & \frac{2Bo\left(-1 + e^{2\sqrt{Bo}} \right) - Bo^{3/2} \left(1 + e^{2\sqrt{Bo}} \right) C_V}{2\left(1 + \sqrt{Bo} + \left(-1 + \sqrt{Bo} \right) e^{2\sqrt{Bo}} \right)} + \\ & + \frac{\sqrt{Bo}\, c\, DEP \sqrt{\pi} \left(\left(1 + e^{2\sqrt{Bo}} \right) Erf\left[\frac{1}{c} \right] - e^{\sqrt{Bo} + \frac{Boc^2}{4}} \left(Erf\left[\frac{1}{c} - \frac{\sqrt{Bo}c}{2} \right] + Erf\left[\frac{1}{c} + \frac{\sqrt{Bo}c}{2} \right] \right) \right)}{2\left(1 + \sqrt{Bo} + \left(-1 + \sqrt{Bo} \right) e^{2\sqrt{Bo}} \right)}. \end{aligned} \qquad \text{[S2.7]}$$

To present a simplified solution we solve for the case of $Bo = 0$ and also assume an initially flat interface, i.e., $C_V = 2$, which simplifies the solution even further. The Bond number in our system is not negligible $Bo \approx 10$ yet, the solution for the deformation of the simplified case with initially flat interface,

$$d(\xi) = A\left(\left(-8\mathrm{e}^{-\frac{\xi^2}{c^2}} + 2\mathrm{e}^{-\frac{1}{c^2}}\left(1+3\xi^2\right)\right)c + \sqrt{\pi}\left(\left(2+6\xi^2-3c^2\left(\xi^2-1\right)\right)\mathrm{erf}\left[\frac{1}{c}\right] - 8\xi\,\mathrm{erf}\left[\frac{\xi}{c}\right]\right)\right), \qquad [S2.8]$$

yielding decent approximation for the realistic case as presented in Fig. S3. Thus, because the Bond number, i.e., the gravity effect on the system, indeed alter the initial shape of the fluid. However, when examining the deformation, we subtract the initial shape from the shape of the interface after actuation. This way, in order to test the importance of gravity in the system, one needs to compare the Bond number with the DEP number while choosing an appropriate scaling to the length scale such as the width of the DEP force distribution.

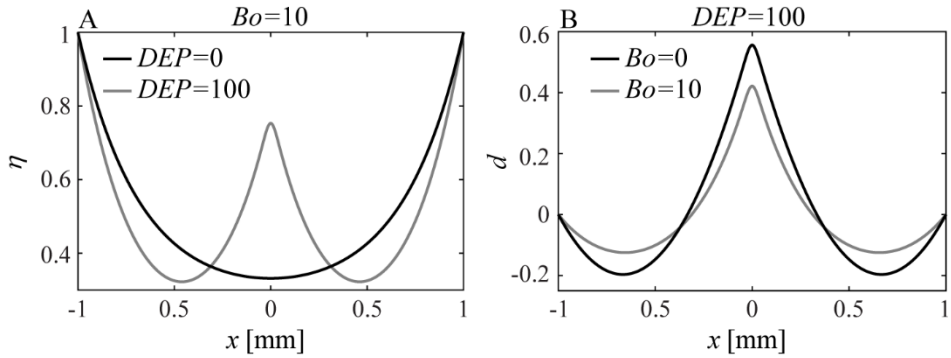

Fig. S3. *Solutions for the DEP induced deformations of the interface using pair of electrode configuration with and without the effect of gravity for typical non-dimensional actuation and Bond number values. (A) The shape of the interface before (black solid line) and after (gray solid line) actuation for* $Bo = 10$. *(B) Comparision of the induced deformations with (gray solid line) and without (black solid line) gravity for* $DEP = 100$. *The black line represents the deformations of the interface for the initialy flat case, solution of equation.*[S2.5]*, and the gray line represents the deformation the interface presented in A, i.e., substracting the initial shape of the interface from the inteface shape after actuation.*

3. DHM measurements interpretation

Digital holography microscopy (DHM) is a holography method which records a hologram image on a digital sensor, i.e., CCD or CMOS camera. The reconstruction of the image is done using numerical algorithms allowing fast acquisition and reconstruction of holograms in real-time. In this work we used the Lyncee Tec R1003 is a DHM working in reflection mode. In this mode the phase shift of the wave reflected from the measured surface is reconstructed using the hologram image.

In our experimental setup the liquid film is very thin, thus when we try to focus on the liquid-air interface, the floor of the chamber (the electrodes surface) is still in the coherence length of the microscope (the coherence length of the DHM is $200\,\mu\text{m}$). Thus, data gathered from the liquid-air interface contains interference pattern resulting from the floor. Moreover, the bottom surface consists of areas which are only glass, and areas of glass covered with $6\,\text{nm}$ of metal (the electrodes) which creates distortions of the measurements above the electrodes. To overcome this issue, we work in "semi-reflective mode", in which we focus on the very last surface in our device, the back side of the glass, and by the phase shift measurements obtained from this surface we calculate the surface topography.

Figure S4 presents schematic illustration of the two working modes. In the regular reflection mode, we can write the phase shift of the two beams and the difference between them as,

$$\begin{aligned} &\varphi_1 = 2\frac{2\pi}{\lambda}h_1 n_a, \quad \varphi_2 = 2\frac{2\pi}{\lambda}h_2 n_a \\ &\Delta\varphi = \varphi_2 - \varphi_1 = 2\frac{2\pi}{\lambda}n_a\left(h_2 - h_1\right) = 2\frac{2\pi}{\lambda}n_a\Delta h \end{aligned} \qquad \text{[S3.1]}$$

where h and φ represents the distance of the surface from the objective and the phase shift of the reflected beam respectively, λ is the wavelength of the laser beam and n_a is the refractive index of the air. To calculate the surface topography, we multiply the phase shift data obtain from the DHM by the following conversion factor,

$$\Delta h = \underbrace{\frac{\lambda}{4\pi n_a}}_{\substack{\textit{Conversion}\\ \textit{factor}}} \cdot \Delta\varphi\,. \qquad \text{[S3.2]}$$

This conversion factor is one of the data the DHM provides when measuring a surface topography. However, if one focus on the lower surface as explained above, this factor needs to be modified. Based on the same process we did for the reflective mode we write the phase shift and phase difference of the two beams except for the location of the reference surface, which is now the bottom surface,

$$\begin{aligned} &\varphi_1 = 2\frac{2\pi}{\lambda}h_1 n_a + 2\frac{2\pi}{\lambda}t n_f, \quad \varphi_2 = 2\frac{2\pi}{\lambda}h_2 n_a + 2\frac{2\pi}{\lambda}\left(t - \Delta h\right)n_f \\ &\Delta\varphi = \frac{4\pi}{\lambda}\left(h_2 n_a - \Delta h n_f - h_1 n_a\right) = \frac{4\pi\left(n_a - n_f\right)}{\lambda}\Delta h \end{aligned} \qquad \text{[S3.3]}$$

where t and n_f are the smallest thickness and the refractive index of the transparent matter as illustrated in Figure 4SB. We note that although the beams reach the bottom surface, the thickness of the transparent matter is, t, cancel out from the equation. For that reason, adding more transparent layers with uniform thickness does not alter the conversion factor of our semi-reflective configuration,

$$\Delta h = \underbrace{\frac{\lambda}{4\pi\left(n_a - n_f\right)}}_{\substack{Conversion \\ factor}} \cdot \Delta\varphi \qquad [S3.4]$$

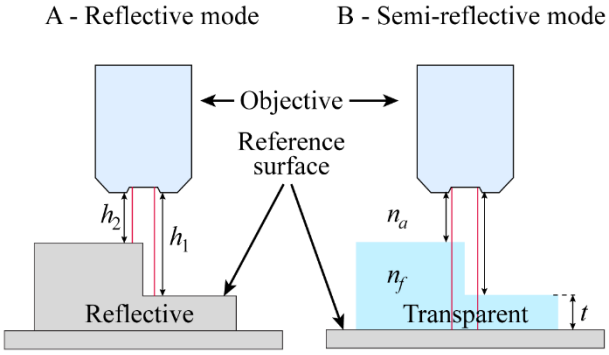

Fig. S4. *Schematic illustration of the reflective and the semi reflective modes measuring the exact same topography made of reflective and transparent matters. The distance between the objective and the surface are* h_1 *and* h_2 *for the farther and closer surface to the objective respectively and* t *is the distance thickness of the smaller step.* n_a *and* n_f *are the refractive indices of the transparent matter and the air, respectively. (A) present the normal working mode of the DHM where we focus on the surface we wish to measure and (B) presents the Semi-reflective mode where the focus is on different surface located below the interface we wish to measure.*

4. Surface Roughness measurements using the digital holographic microscope

We measure the surface topography of an atomically polished silicon wafer with surface roughness of sub nanometer. By examine a field of view of $50 X 50 \mu m^2$ (containing 86X86 data points), we yield a surface roughness with an RMS value of $3.7\,nm$ using the digital holography microscope. Thus, showing the limit of the DHM as a measurement tool for surface quality.

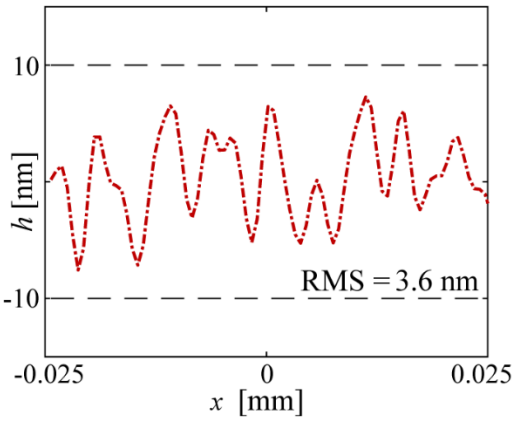

Fig. S5. *Typical cross section measurement (* $50\,\mu m$ *in length) of an atomically polished wafer for estimation of the surface quality measurements capabilities using the DHM, yielding an RMS value of* $3.6\,nm$.

5. Captions for the Movies

Movie S1. Y – junction deformation. *A microfluidic chamber and filled with silicone oil and patterned with electrodes pairs forming an outline of a Y-junction. Upon activation, the deformation is rapidly formed, can be easily modulated in amplitude, turned on and off, and quickly recovers from external forced disturbances.*

Movie S2. Dynamic modulation of parallel-electrodes array. *A chamber containing array of 16 parallel-electrodes. The chamber filled with silicone oil and by setting an electric potential to one electrodes pair at a time we create a propagating wave and introduced for the first time our novel micro piano.*

6. SI references

Leal, L. G. (2007). *Advanced Transport Phenomena: Fluid Mechanics and Convective Transport Processes.* Cambridge University Press. http://public.eblib.com/choice/publicfullrecord.aspx?p=667626

Melcher, J. R. (1981). *Continuum electromechanics*. MIT Press.

Oron, A., Davis, S. H., & Bankoff, S. G. (1997). Long-scale evolution of thin liquid films. *Reviews of Modern Physics*, *69*(3), 931–980. https://doi.org/10.1103/RevModPhys.69.931

Stratton, J. A. (1941). *Electromagnetic Theory*. McGraw-Hill.